Astronomy & Astrophysics manuscript no. preprint
December 30, 2011

Searching for the first stars with the Gaia mission

R. S. de Souza[1,2], A. Krone-Martins[3], E.E.O. Ishida[1,2], and B. Ciardi[4]

[1]IAG, Universidade de São Paulo, Rua do Matão 1226, 05508-900, São Paulo, SP, Brazil
[2]IPMU, University of Tokyo, 5-1-5 Kashiwanoha, Kashiwa, Chiba 277-8583, Japan
[3]SIM, Faculdade de Ciências, Universidade de Lisboa, Ed. C8, Campo Grande, 1749-016, Lisboa, Portugal
[4]Max-Planck-Institut für Astrophysik, Karl-Schwarzschild-Str. 1, D-85748 Garching, Germany

Released Xxxxx XX

ABSTRACT

Aims. We construct a theoretical model to predict the number of orphan afterglows (OA) from gamma-ray bursts (GRBs) triggered by primordial metal free (Pop III) stars expected to be observed by the Gaia mission. In particular, we consider primordial metal free stars which were affected by radiation from other stars (Pop III.2) as a possible target.
Methods. We use a semi-analytical approach, with the inclusion of all relevant feedback effects, to construct the cosmic star formation history and its connection with GRBs cumulative number. The OA events are generated via Monte-Carlo method, and realistic simulations of Gaia's scanning law are performed to derive the observation probability expectation.
Results. We show that $\sim 0.4\%$ of all Pop III.2 afterglows should appear in the sky above of Gaia observational flux limit. Combining this result with simulations of Gaia's scanning law, we expect to observe an average of $\sim 13\% \pm 7\%$ of all OA above the observational sensitivity.

Key words. Stars: Population III; Gamma-ray burst; Gaia mission

1. Introduction

The first stars in the Universe are thought to have played a crucial role in the early cosmic evolution, by emitting the first light and producing the first heavy elements (Bromm et al. 2009). The understanding of such objects is of great importance, since their detection would permit to probe the pristine regions of the Universe. However, there has been no direct observation of the so-called Population III (hereafter, Pop III-primordial metal free) stars up to now.

Pop III stars may produce collapsar gamma-ray bursts (GRBs) whose total isotropic energy could be $\approx$ 2 orders of magnitude larger than average (Barkov 2010; Komissarov & Barkov 2010; Mészáros & Rees 2010; Suwa & Ioka 2011; Toma et al. 2011). Even if the Pop III star has a supergiant hydrogen envelope, the GRB jet can break out of it because of the long-lasting accretion of the envelope itself (Nagakura et al. 2011; Suwa & Ioka 2011). It is of great importance to study the rate and detectability of Pop III GRBs prompt emissions, as well as their afterglows, by current and future surveys. We explore here the possibility to observe these objects through their afterglows (Toma et al. 2011). Observations of GRBs afterglows make it possible to derive physical properties of the explosion mechanism and the circumburst medium. It is intriguing to search for signatures of metal poor stars in the GRB afterglows at low and high redshifts.

GRB optical afterglows are one of the possible transients to be detected by the Gaia[1] mission. Recently Japelj & Gomboc (2011) have explored the detectability of such afterglows with Gaia using a Monte-Carlo approach that inspired us. As the GRB jet sweeps the interstellar medium, the Lorentz factor of the jet is decelerated and the jet starts to expand sideways, eventually becoming detectable by off-axis observers. These afterglows are not associated with the prompt GRB emission and are called orphan afterglows (OA) (Nakar et al. 2002; Rossi et al. 2008).

de Souza et al. (2011) showed that, considering EXIST[2] specifications, we can expect to observe a maximum of $\approx$ 0.08 GRBs with $z > 10$ per year originated from primordial metal free stars (Pop III.1) and $\approx$ 20 GRBs with $z > 6$ per year coming from primordial metal

Send offprint requests to: Rafael S. de Souza e-mail: `rafael@astro.iag.usp.br`

---

[1] http://www.rssd.esa.int/GAIA/
[2] http://exist.gsfc.nasa.gov/design/

free stars which were affected by the radiation from other stars (Pop III.2). In the context of the current *Swift*[3] satellite, ≈ 0.2 GRBs with $z > 6$ per year from Pop III.2 stars are expected. These numbers reflect the fact that, compared to PopIII.1 stars, Pop III.2 stars are more abundant and can be observed in a lower redshift range, which makes them more suitable targets. In the light of such results, the calculations presented here will focus on Pop III.2 stars alone.

Orphans afterglows have been searched by both X-ray surveys (Grindlay 1999; Greiner et al. 2000) as well as by optical searches (Becker et al. 2004; Rykoff et al. 2005; Rau et al. 2006; Malacrino et al. 2007). The purpose of the present paper is to calculate the Pop III.2 GRB orphan afterglows rate that might be detected by the Gaia mission (for more details about Gaia, see e.g., Perryman et al. 2001; Lindegren 2009).

The Gaia mission is one of the most ambitious projects of modern Astronomy. It aims at the creation of a very precise tridimensional, dynamical and chemical census of our Galaxy, from astrometric, spectrophotometric and spectroscopic data. In order to do so, the Gaia satellite will perform observations of the entire sky in a continuous scanning created from the coupling of rotations and precessions movements called 'scanning law'. For point-sources, these observations will be unbiased and the data of all the objects under a certain limiting magnitude (G=20), will be transferred to the ground. Certainly, among all those objects, not only galactic sources will be present, but also extragalactic ones.

Typically, Pop III.2 stars are formed in an initially ionized gas (Johnson & Bromm 2006; Yoshida et al. 2007). They are thought to be less massive than Pop III.1 stars but still massive enough for producing GRBs. Recent results from Greif et al. (2011), show that instead of forming a single object, the gas in minihalos fragments vigorously into a number of protostars with a range of different masses. It's not clear up to now how this initial range of mass will be mapped into the final mass function of Pop III stars. The most likely conclusion is that Pop III stars are less likely to reach masses in excess of $\sim 140 M_{\odot}$, which consequently affect the number of GRBs from Pop III.1 usually estimated. Here we assume that this will not affect significantly the mass range assumed for Pop III.2 ($\sim 40 - 100 M_{\odot}$).

The paper is organized as follows. In Sect. 2, we calculate the formation rate of primordial GRBs. In Sect. 3, we calculate the orphan afterglow light curves and their redshift distribution. In Sect. 4, we derive the probability of a given event to be observed by Gaia. In Sect. 5 we discuss the results and give our concluding remarks. Throughout the paper we adopt the standard Λ Cold Dark Matter model with the best fit cosmological parameters from Jarosik et al. (2011) (WMAP-Yr7[4]), $\Omega_{\rm m} = 0.267, \Omega_{\Lambda} = 0.734$, and $H_0 = 71 {\rm km\ s^{-1} Mpc^{-1}}$.

2. GRB redshift distribution

To estimate the formation rate of GRBs from Pop III stars at a given redshift we closely follow de Souza et al. (2011). Since long GRBs are expected to follow the death of very massive stars, their rate could provide an useful probe for cosmic star formation history (e.g., Totani 1997; Ciardi & Loeb 2000; Bromm & Loeb 2002; Conselice et al. 2005; Campisi et al. 2010, 2011a; Ishida et al. 2011; de Souza et al. 2011; Robertson & Ellis 2012). However, the connection between the star formation rate density (SFR) and GRB rate is not clearly understood and can be redshift dependent (e.g., Yüksel et al. 2008; Kistler et al. 2009; Robertson & Ellis 2012). Several studies connect the origin of long GRBs with the metallicity of their progenitors (e.g., Mészáros 2006; Woosley & Bloom 2006; Salvaterra & Chincarini 2007; Salvaterra et al. 2009; Campisi et al. 2011b), since host galaxies of long duration GRBs are often observed to be metal poor. Consequently the GRB-SFR connection could be dependent of the cosmic metallicity evolution. However, such connection is not completely understood yet, since there is also evidence of regions within GRB host galaxies known to posses higher metallicities (Levesque et al. 2010).

Despite such uncertainties, because Pop III stars as well as their environment are metal poor, we expect the connection between SFR and GRBs to be less affected by this effect. In other words, Pop III stars are more likely to produce GRBs than ordinary stars. It's important to keep in mind that any prediction will be convolved with systematic effects that we are not taking into account. However, as pointed out in Ishida et al. (2011), the assumption is good enough to agree with available observational data.

We implicitly assume that the formation rate of long GRBs (duration longer than 2 sec) follows closely the star formation history (SFH) (e.g., Totani 1997; Campisi et al. 2010; Ciardi & Loeb 2000; Campisi et al. 2011a; Conselice et al. 2005; Bromm & Loeb 2006; de Souza et al. 2011; Ishida et al. 2011). The number of GRBs per comoving volume per time can be expressed as

$$\Psi_{\rm GRB}(z) = \eta_{\rm GRB} \Psi_*(z), \tag{1}$$

where $\eta_{\rm GRB}$ is the GRB formation efficiency and Ψ_* is the SFR. Over a particular time interval, $\Delta t_{\rm obs}$, in the observer rest frame, the number of GRBs originating between redshifts z and $z + dz$ is

$$\frac{{\rm d}N_{\rm GRB}}{{\rm d}z} = \Psi_{\rm GRB}(z) \frac{\Delta t_{\rm obs}}{1+z} \frac{{\rm d}V}{{\rm d}z}, \tag{2}$$

where ${\rm d}V/{\rm d}z$ is the comoving volume element per redshift unit.

2.1. Star Formation History

To estimate the SFR at early epochs, we assume that stars are formed in collapsed dark matter halos (for

---

[3] http://swift.gsfc.nasa.gov/docs/swift/swiftsc.html

[4] http://lambda.gsfc.nasa.gov/product/map/current/

more details, please see de Souza et al. 2011). The number of collapsed objects is given by the halo mass function (Hernquist & Springel 2003; Greif & Bromm 2006; Trenti & Stiavelli 2009). In what follows, we adopt the Sheth-Tormen one, f_{ST}, (Sheth & Tormen 1999). To estimate the fraction of mass inside each halo able to collapse and form stars we include all important feedback mechanisms described next.

1. H_2 Photodissociation
   Hydrogen molecules (H_2) are the primary coolant in the gas within small mass “minihalos”. H_2 are also fragile to ultra-violet radiation in the Lyman-Werner (LW) bands and can easily be suppressed by it. We model the dissociation effect by setting the minimum mass for halos that are able to host Pop III stars (Yoshida et al. 2003).
2. Reionization
   Inside growing HII regions, the gas is highly ionized and the temperature is $\sim 10^4$ K. The volume filling factor of ionized regions, $Q_{\mathrm{HII}}(z)$, determines when the formation of Pop III.1 stars is terminated and switches to Pop III.2. To calculate $Q_{\mathrm{HII}}(z)$, we closely follow Wyithe & Loeb (2003) as in de Souza et al. (2011).
3. Metal Enrichment
   The metal-enrichment in the inter-galactic medium (IGM) determines when the formation of primordial stars is terminated (locally) and switches from the Pop III mode to a more conventional mode of star formation. We assume that star-forming halos launch a wind of metal-enriched gas at $z \gtrsim 20$. Then we follow the metal-enriched wind propagation outward from a central galaxy with a given velocity v_{wind}, traveling over a comoving distance R_{wind}. We estimate the ratio of gas mass enriched by the wind to the total gas mass in each halo and then we evaluate the average metallicity over cosmic scales as a function of redshift. We effectively assume that the so-called critical metallicity is very low (Schneider et al. 2002, 2003; Bromm & Loeb 2003; Omukai et al. 2005; Frebel et al. 2007; Belczynski et al. 2010). Therefore, Pop III stars are not formed in a metal-enriched region, regardless of the actual metallicity.

The top panel of Fig. 1 shows the upper limit for Pop III.2 SFR derived in de Souza et al. (2011). The Pop III.2 SFR is compared with a compilation of independent measures from Hopkins & Beacom (2006) up to $z \approx 6$ and from observations of color-selected Lyman Break Galaxies (Mannucci et al. 2007; Bouwens et al. 2008, 2011), Lyα Emitters (Ota et al. 2008), UV+IR measurements (Reddy et al. 2008), and GRB observations (Chary et al. 2007; Yüksel et al. 2008; Wang & Dai 2009) at higher z (in the figure, these will be refereed to as H2006, M2007, B2008, B2011, O2008, R2008, C2007, Y2008 and W2009, respectively).

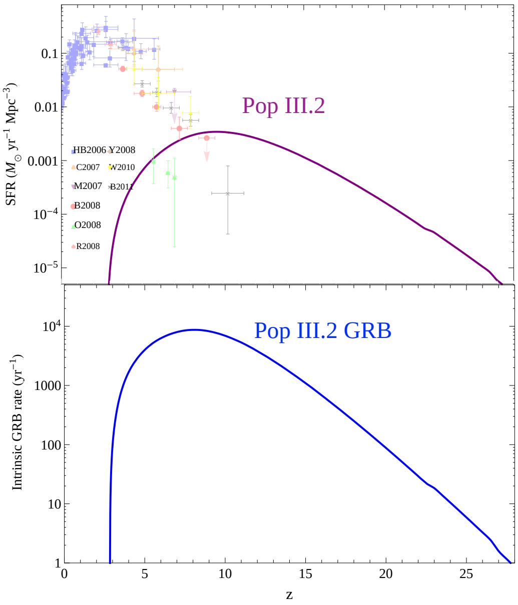

Fig. 1. Top: Optimistic model for Pop III.2 star formation rate assuming a high star formation efficiency and low chemical enrichment. The light points are independent SFR determinations compiled from the literature. Bottom: The intrinsic GRB rate $\mathrm{d}N_{\mathrm{GRB}}/\mathrm{d}z$. In other words, the number of GRBs per year on the sky (on-axis + off-axis) according to Eq. (2). This represents our optimistic model assuming a high star formation efficiency for Pop III.2, slow chemical enrichment, GRB formation efficiency of $f_{GRB} = 0.01$ and a Salpeter IMF.

2.2. *Initial Mass Function and GRB Formation Efficiency*

The stellar initial mass function (IMF) is critically important to determine the Pop III GRB rate. The IMF determines the fraction of stars with minimum mass that is able to trigger GRBs, $\sim 25 M_\odot$ (Bromm & Loeb 2006). The f_{GRB} factor gives the fraction of stars in this range of mass that will produce GRBs.

The GRB formation efficiency factor per stellar mass is

$$\eta_{\mathrm{GRB}} = f_{\mathrm{GRB}} \frac{\int_{M_{\mathrm{GRB}}}^{M_{\mathrm{up}}} \phi(m) dm}{\int_{M_{\mathrm{low}}}^{M_{\mathrm{up}}} m\phi(m) dm}, \tag{3}$$

where $\phi(m)$ is the stellar IMF for which we considered a power law with the standard Salpeter slope $\phi(m) \propto m^{-2.35}$, M_{low} and M_{up} are the minimum and maximum mass for a given stellar type (respectively $10 M_\odot$ and $\sim 100 M_\odot$ for Pop III.2). M_{GRB} is the minimum mass able to trigger GRBs, which we set to be $25 M_\odot$ (Bromm & Loeb 2006).

de Souza et al. (2011) placed upper limits on the intrinsic GRB rate (including the off-axis GRB). In what follows, we set $f_{GRB} = 0.01$ and $\eta_{\mathrm{GRB}}/f_{\mathrm{GRB}} \sim 1/87 M_\odot^{-1}$ as an optimistic case, consistent with their results. The bottom panel of Fig. 1 shows the upper limit for intrinsic GRB rate derived in de Souza et al. (2011).

3. Number of Observed Orphans

3.1. Afterglow Model

To calculate the afterglow light curves of Pop III GRBs we follow the standard prescription from Sari et al. (1998, 1999) and Mészáros (2006). The spectrum consists of power-law segments linked by critical break frequencies. These are $\nu_{\rm a}$ (the self absorption frequency), $\nu_{\rm m}$ (the peak of injection frequency) and $\nu_{\rm c}$ (the cooling frequency), given by

$$\begin{aligned}
\nu_{\rm m} &\propto (1+z)^{1/2} g(p)^2 \epsilon_e^2 \epsilon_B^{1/2} E_{\rm iso}^{1/2} t_d^{-3/2}, \\
\nu_{\rm c} &\propto (1+z)^{-1/2} \epsilon_B^{-3/2} n^{-1} E_{\rm iso}^{-1/2} t_d^{-1/2}, \\
\nu_{\rm a} &\propto (1+z)^{-1} \epsilon_e^{-1} \epsilon_B^{1/5} n^{3/5} E_{\rm iso}^{1/5}, \\
F_{\nu,\max} &\propto (1+z) \epsilon_B^{1/2} n^{1/2} E_{\rm iso} d_L^{-2}, \qquad (4)
\end{aligned}$$

where $g(p) = (p-2)/(p-1)$ is a function of the energy spectrum index of electrons ($N(\gamma_e)d\gamma_e \propto \gamma_e^{-p} d\gamma_e$, where γ_e is the electron Lorentz factor), ϵ_e and ϵ_B are the efficiency factors (Mészáros 2006) and $F_{\nu,\max}$ is the observed peak flux at luminosity distance d_L from the source.

There are two types of spectra. If $\nu_{\rm m} < \nu_{\rm c}$, we call it the *slow cooling case*. The flux at the observer, F_ν, is given by

$$F_\nu = \begin{cases} (\nu_{\rm a}/\nu_{\rm m})^{1/3} (\nu/\nu_{\rm a})^2 F_{\nu,\max}, & \nu_{\rm a} > \nu, \\ (\nu/\nu_{\rm m})^{1/3} F_{\nu,\max}, & \nu_{\rm m} > \nu > \nu_{\rm a}, \\ (\nu/\nu_{\rm m})^{-(p-1)/2} F_{\nu,\max}, & \nu_{\rm c} > \nu > \nu_{\rm m}, \\ (\nu_{\rm c}/\nu_{\rm m})^{-(p-1)/2} (\nu/\nu_{\rm c})^{-p/2} F_{\nu,\max}, & \nu > \nu_{\rm c}. \end{cases} \qquad (5)$$

For $\nu_{\rm m} > \nu_{\rm c}$, called the *fast cooling case*, the spectrum is

$$F_\nu = \begin{cases} (\nu_{\rm a}/\nu_{\rm c})^{1/3} (\nu/\nu_{\rm a})^2 F_{\nu,\max}, & \nu_{\rm a} > \nu, \\ (\nu/\nu_{\rm c})^{1/3} F_{\nu,\max}, & \nu_{\rm c} > \nu > \nu_{\rm a}, \\ (\nu/\nu_{\rm c})^{-1/2} F_{\nu,\max}, & \nu_{\rm m} > \nu > \nu_{\rm c}, \\ (\nu_{\rm m}/\nu_{\rm c})^{-1/2} (\nu/\nu_{\rm m})^{-p/2} F_{\nu,\max}, & \nu > \nu_{\rm m}. \end{cases} \qquad (6)$$

Initially the jet propagates as if it were spherical with an equivalent isotropic energy of $E_{\rm true} = \theta_j^2 E_{\rm iso}/2$, where θ_j is the half opening angle of the jet. Even if the prompt emission is highly collimated, the Lorentz factor drops $\gamma_{\rm d} < \theta_j^{-1}$ around the time

$$t_\theta \sim 2.14 \left(\frac{E_{\rm iso}}{5\times 10^{54}}\right)^{1/3} \left(\frac{\theta_j}{0.1}\right)^{8/3} n^{-1/3} (1+z) \text{ days}, \qquad (7)$$

and the jet starts to expand sideways (Ioka & Mészáros 2005). Consequently, the jet becomes detectable by the off-axis observers. These afterglows are not associated with the prompt GRB emission.

Due to relativistic beaming, an observer located at θ_{obs}, outside the initial opening angle of the jet ($\theta_{obs} > \theta_j$), will observe the afterglow emission only at $t \sim t_\theta$, when $\gamma_{\rm d} = \theta_j^{-1}$.

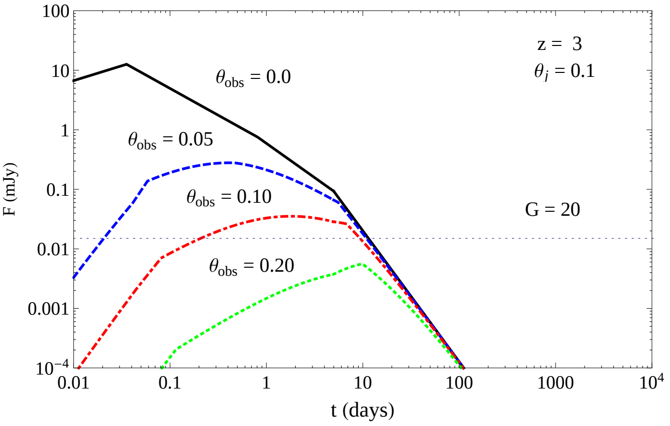

Fig. 2. Example of afterglow light curve at $z = 3$ as a function of observed angle, θ_{obs}. We show the evolution of afterglow flux $F(mJy)$ as a function of time t (days) and observed angle θ_{obs} for typical parameters: isotropic kinetic energy $E_{iso} = 10^{54}$ erg, electron spectral index $p = 2.5$, plasma parameters $\epsilon_e = 0.1$, $\epsilon_B = 0.01$, half opening angle jet $\theta_j = 0.1$, interstellar medium density $n = 1cm^{-3}$ and frequency $\nu = 5 \times 10^{14}$Hz. The horizontal dotted line is the integrated Gaia flux limit; solid black line, $\theta_{obs} = 0$; dashed blue line, $\theta_{obs} = 0.05$; dot-dashed red line, $\theta_{obs} = 0.1$; dotted green line, $\theta_{obs} = 0.20$.

The received afterglow flux by an off-axis observer in the point source approximation, valid for $\theta_{obs} \gg \theta_j$, is related to that seen by an on-axis observer, by (Granot et al. 2002; Totani & Panaitescu 2002; Japelj & Gomboc 2011)

$$F_\nu(\theta_{obs}, t) = \xi^3 F_{\nu/\xi}(0, \xi t), \qquad (8)$$

where

$$\xi \equiv (1-\beta)/(1-\beta\cos\theta_{obs}), \qquad (9)$$

and $\beta = \sqrt{1 - 1/\gamma_{\rm d}^2}$. The time evolution of the Lorentz factor in given by

$$\gamma_{\rm d}(t) = \begin{cases} \theta_{\rm j}^{-1} \left(\frac{t}{t_{\rm j}}\right)^{-3/8} & t < t_{\rm j} \\ \theta_{\rm j}^{-1} \left(\frac{t}{t_{\rm j}}\right)^{-1/2} & t > t_{\rm j}. \end{cases} \qquad (10)$$

Fig. 2 shows four examples of afterglows as a function of observed angle θ_{obs} for the case of $\theta_j = 0.1$ at $z = 3$ for typical parameters described in the figure. The flux is calculated for an observational frequency $\nu = 5 \times 10^{14}$Hz within the Gaia bandwith. Depending on the parameters of the afterglow, the light curve can appear above the Gaia observational limits. Due to the large quantity of free parameters, a Monte-Carlo approach is essential to explore the detectability of a large amount of events and will be explained in the next section.

3.2. Mock sample

The mock sample is generated by a Monte-Carlo method assuming different probability distribution functions (PDF) for each quantity as explained below.

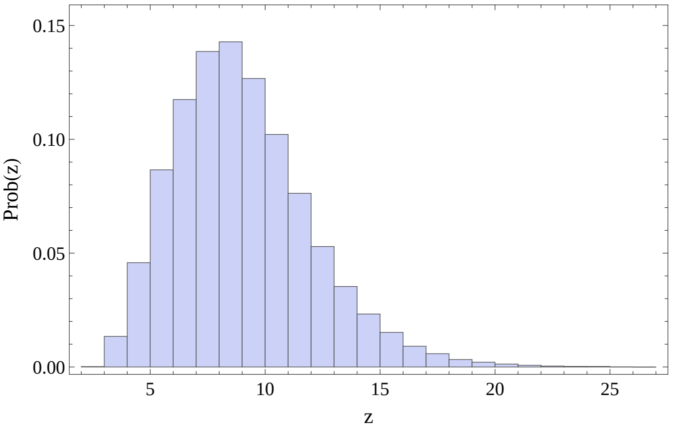

Fig. 3. Redshift PDF. Probability of a given event to appear in a certain range of redshift.

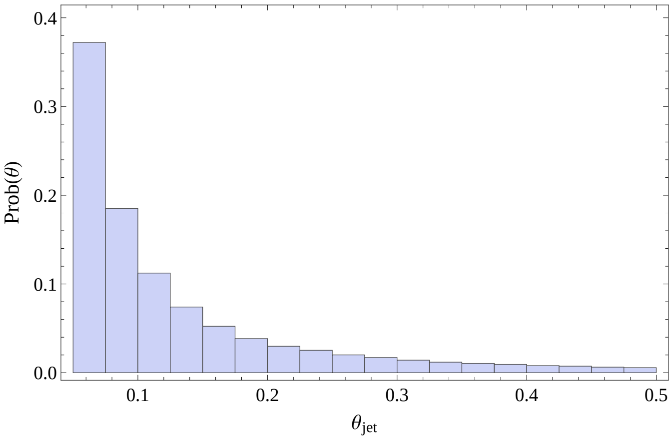

Fig. 4. Half opening angle jet PDF. Probability of a given GRB to have a particular θ_j.

3.2.1. Redshift PDF

We generate the GRB events randomly in redshift with a PDF given by Eq. (2). The probability of a given GRB to appear at redshift z is

$$P_z(z) = \frac{dN_{GRB}/dz}{\int_0^z (dN_{GRB}/dz)dz}. \tag{11}$$

The PDF was generated by 10^5 random realizations based on Eqs. (2) and (11). Fig. 3 shows the probability to find a GRB at a given redshift, indicating that a 50% of probability to have a GRB from a PopIII star is obtained in the redshift range $z \sim 7-11$ and 95% in the range $z \sim 4-15$.

3.2.2. Half opening angle PDF

Using an empirical opening angle estimator, Yonetoku et al. (2005) derived the opening angle PDF of GRBs. Their PDF can be fitted by a power-lay θ^{-2} with a cut off at $\sim$ 0.04. Their results seem also compatible with the universal structured jet model (Perna et al. 2003). For simplicity, we assume a similar power-law in the range $\theta_j^{min} = 0.05$ and $\theta_j^{max} = 0.5$ to determine the PDF of θ_j,

$$P_{\theta_j(\theta)} \propto \theta^{-2}. \tag{12}$$

Fig. 4 shows the PDF of θ_j generated by 10^5 realizations based on Eq. (12). The realizations were performed within the range $\theta_j = 0.05 - 0.5$. The observational angle, θ_{obs}, was randomly chosen between $0 - \pi$.

4. The Gaia mission

The Gaia satellite will perform observations of the entire sky, using a continuous scanning formed by the coupling of rotation and precession movements - the ‘scanning law’. This law guarantees that each point in the sky will be observed several times during the mission, as it can be seen in Fig. 5.

Similar to what happens with CCD meridian circles, in the referential of the satellite’s focal plane the sky continuously moves from one side to the other while the satellite spins. During all the time, the CCD charges are synchronously transferred, as to compensate the apparent sky’s motion and allow the integration.

This continuous observation strategy requires an equally continuous reading of the CCDs. Also, since Gaia’s focal plane comprises 106 individual detectors[5], it is not possible to transfer the entire content of the focal plane to the Earth due to bandwidth limits. So, a continuous analysis of the focal plane observations is also performed on-board, aimed at the detection of astronomical sources. When a source is detected, a rectangular “window” comprising a few arcseconds around the detected source is created (its exact size and pixel binning depends on the focal plane’s CCD column). These “windows” are then transferred to the Earth.

For point-sources, these observations will be unbiased and the data from all objects in the sky, under a certain limiting magnitude, will be sent to the ground. Certainly, among all those objects, not only galactic sources will be present, but also extragalactic ones. In particular, it is expected that point-sources up to magnitude 20, in the Gaia passband G[6], will be “windowed” and transferred[7].

As seen in Fig. 2, some of the orphan events are expected to remain above this limiting magnitude for a certain amount of time. The question that remains is if their duration (at G$\leqslant$20) is enough for them to be observed at a reasonable rate. In order to estimate the probability for

---

[5] For a diagram of Gaia’s focal plane, see for ex. Jordi et al. (2010).

[6] This is a broad passband, which covers from 330-1000 nm. The nominal transmission curve can be found at Jordi et al. (2010).

[7] After the mission (and during the mission for some problematic cases), it will be possible to reconstruct a deeper image around each detected source. In those reconstructed images, it will be possible to reach deeper magnitudes, albeit with some contamination from reconstruction artifacts.

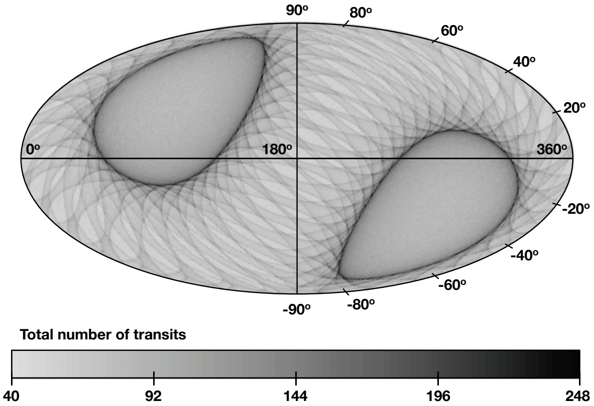

Fig. 5. Number of times each region of the sky (in galactic coordinates) will be observed by the Gaia satellite during the entire mission.

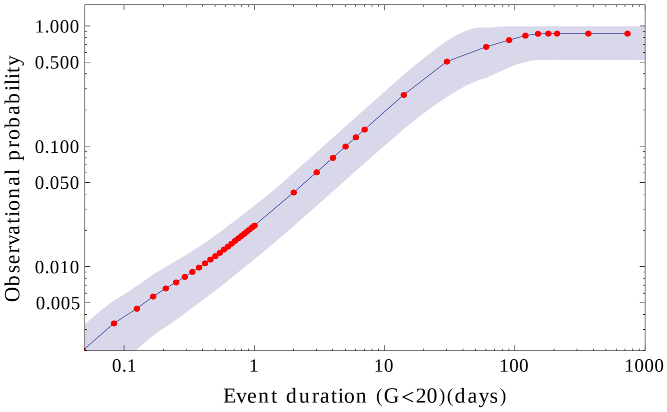

Fig. 6. Probability for a transient event with duration Δt to be observed by Gaia. Δt is the time the event stays brighter than the Gaia limiting magnitude during the 5 years nominal mission.

the observation of a single event from a Pop III.2 by Gaia, only two quantities play an important role: the time which the orphan remains brighter than G=20, Δt, and the coordinates (l_{gal}, b_{gal}) where the event takes place in the sky. Since those quantities are continuous distributions, it is necessary to analyze how the observation probability depends on them, building $P(\Delta t, l_{gal}, b_{gal})$. In the present work, we proceed as follows.

For a given coordinate in the sky, we start by computing the inverse Gaia scanning law as to derive a transit time list comprising the instants when Gaia's telescopes will be pointing at that coordinate. In order to be as realistic as possible, we adopt the Gaia Data Processing and Analysis Consortium's nominal implementation of it. Then, we randomly select a point in time during the entire mission lifetime in order to place an event of a certain duration Δt. Using the transit time list we check if that event was observed, considering a time window of 4.4 seconds around each transit - this is the time needed for the signal to cross the detection CCD and enter the confirmation CCD. If there is a superposition between the event duration and this time window, the event is considered detected. This procedure is then repeated until the estimation of the detection probability, which is derived by simply dividing the number of detected events by the total, does not vary more than 1% between iterations. Finally, the whole procedure is repeated for each event duration Δt. As a consequence, we obtain an adequate time-sampling of the $P(\Delta t, l_{gal}, b_{gal})$ distribution.

For the determination of the number of orphan events observed by Gaia on the entire sky, the coordinate dependency can be averaged out, allowing $P(\Delta t, l_{gal}, b_{gal}) \sim P(\Delta t) \pm \epsilon$. This is possible because the scanning law is mostly known and then we can reasonably assume that the orphan events take place randomly in the sphere.

The procedure described above was repeated for several positions on the sphere, and the mean and the standard deviation at each event duration were computed. To allow a good spatial sampling for the estimation of $P(\Delta t) \pm \epsilon$, we tessellate the celestial sphere at the Hierarchical Triangular Mesh level 4 (Kunszt et al. 2001). This means that the simulations were performed at the center of 2048 triangles of approximately equal areas.

Finally, in order to obtain the probabilities for the whole sky, an additional effect must be taken into account: the structure of our own Galaxy. Since the orphans are extragalactic events, the probability of observation at the galactic plane or bulge should be null or very small, due to the extinction and crowding. In this work, we conservatively assumed a null value for the probability of orphans being observed at such regions of the sky (defined here as $|b| \leq 15°$ for $345° \leq l \leq 15°$ and $|b| \leq 5°$ otherwise).

The final results, representing the behavior of $P(\Delta t) \pm \epsilon$ can be seen in Fig. 6.

In accordance with upper limit showed in Fig. 1 and results from de Souza et al. (2011), we expect between $\sim 10^2 - 5 \times 10^4$ events per year. The uncertainties come from our poor understanding about the efficiency with which gas is converted into stars and GRBs are triggered (two unknown factors for Pop III stars). For a good statistics, we create a mock sample of 10^5 events randomly generated by Monte-Carlo method in order to infer the PDF of an event to stay below $G = 20$ over Δt(days). The average behavior is shown in Fig. 7. Since we have $P(\Delta t)$, we can generate a sample with $10^2 - 5 \times 10^4$ events several times and test against their probability of being observed by Gaia given by Fig. 6. Combining Figs. 6 and 7, we obtain as an upper limit for the average number of events observed per year $\sim 26 \pm 14$, and $\sim 0.26 \pm 0.14$ as the lower limit.

5. Conclusion and Discussion

Despite recent developments in theoretical studies on the formation of the early generation of stars, there are no direct observations of Population III stars yet. Following the

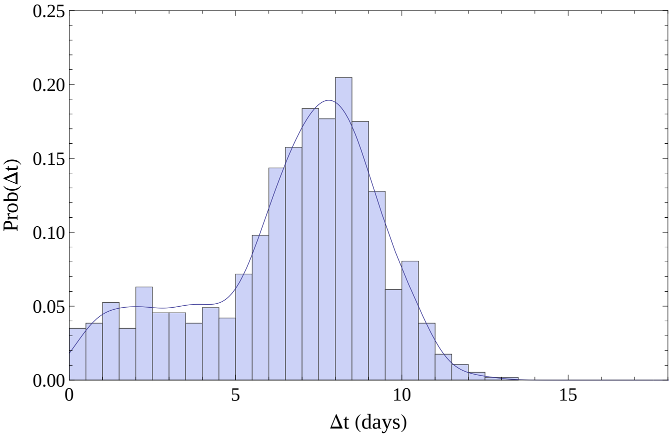

Fig. 7. PDF of $\Delta t(days)$. Probability of an orphan afterglow to appear above the Gaia flux limit for a given time interval.

suggestion that massive Pop III stars could trigger collapsar GRBs, we investigated the possibility to observe their orphan afterglows. We used previous results from the literature to estimate the SFR for Pop III.2 stars, including all relevant feedback effects: photo-dissociation, reionization and metal enrichment.

Since we expect a larger number of orphans than on-axis GRBs, we estimated the possibility to observe such events during the 5 nominal operational years of the Gaia mission. We obtained the average number of events observed per year to be $\sim 26 \pm 14$ as an upper and $\sim 0.26 \pm 0.14$ as a lower limit.

However, the detection of those events among the Gaia data will not be easy. Gaia will observe more than one billion objects all over the sky, and each object will be independently detected around eighty times during the mission, comprising a total of around 10^{12} astrometric, spectrophotometric and spectroscopic observations (after the detection, the observations are multiplexed in the focal plane). One can promptly realize that finding the orphans events among all that data can be a quite challenging task.

A possible way to search such objects within a large survey is looking for signatures of afterglows from Pop III stars. Two important characteristics of these objects are: the total energy of Pop III GRBs can be much higher than those of Pop I/II GRBs and the active duration time of their jet can be much longer than Pop I/II GRB jets, due to the larger progenitor star. So, the detection of GRBs with very high E_{iso} and very long duration could be indicative of such objects (Toma et al. 2011). But the indication should be complemented with the constraint on the metal abundances in the surrounding medium with high resolution IR and X-ray spectroscopy. Since we don't have any observation of these objects we have to rely on theoretical models to compare with data. A way to look for such objects which is worth a future investigation is the use of some automatic light curve classifiers widely used for classification of supernovae and transients in general (Johnson & Crotts 2006; Kuznetsova & Connolly 2007; Poznanski et al. 2007; Rodney & Tonry 2009; Falck et al. 2010; Newling et al. 2011; Richards et al. 2011; Sako et al. 2011). In principle, the theoretical model could work as a training set for the classifier, which would be then applied to surveys to identify possible candidates for further spectroscopically follow up.

In this context, it is important though to emphasize that our knowledge concerning first stars and their GRBs is still quite incomplete. Many of their properties (e.g. characteristic mass, SFR and efficiency to trigger GRBs) are still very uncertain, and more reliable information can only come once a detection is confirmed. Recently, Hosokawa et al. (2011), performing state of the art radiation-hydrodynamics simulations, showed that the typical mass of primordial stars could be $\sim 43 M_{\odot}$, i.e. less massive than originally expected by theoretical models. Their results though are affected by assumptions on the initial conditions. This confirms that we are far away from understanding all characteristics of these objects and any observation would be of paramount importance to improve theoretical models. In case such events are found among Gaia data, valuable physical properties associated to the primordial stars of our Universe and their environment could be constrained.

Acknowledgements. We are happy to thank the very fruitful suggestions and carefully revision of K. Ioka. We also thanks Andrea Ferrara, Andrei Messinger and André Moitinho for helpful discussions. R.S.S. thanks the Brazilian agency FAPESP (2009/05176-4) and CNPq (200297/2010-4) for financial support. This work was supported by World Premier International Research Center Initiative (WPI Initiative), MEXT, Japan. A.K.M. thanks the Portuguese agency FCT (SFRH/BPD/74697/2010) for financial support. E.E.O.I. thanks the Brazilian agencies CAPES (1313-10-0) and FAPESP (2011/09525-3) for financial support. We also thank the Brazilian INCT-A for providing computational resources through the Gina machine, as well as F. Mignard, X. Luri and the Gaia Data Processing and Analysis Consortium Coordination Unit 2 - Simulations for providing the scanning law implementation classes as well as the wrapper for the HTM sphere partitioning method. Finally, we thanks the Scuola Normale Superiore of Pisa and Centro Brasileiro de Pesquisas Fisicas for its hospitality during part of the work on this paper.

References

Barkov, M. V. 2010, Astrophysical Bulletin, 65, 217

Becker, A. C., Wittman, D. M., Boeshaar, P. C., et al. 2004, ApJ, 611, 418

Belczynski, K., Holz, D. E., Fryer, C. L., et al. 2010, The Astrophysical Journal, 708, 117

Bouwens, R. J., Illingworth, G. D., Franx, M., & Ford, H. 2008, ApJ, 686, 230

Bouwens, R. J., Illingworth, G. D., Labbe, I., et al. 2011, Nature, 469, 504

Bromm, V. & Loeb, A. 2002, ApJ, 575, 111

Bromm, V. & Loeb, A. 2003, Nature, 425, 812

Bromm, V. & Loeb, A. 2006, ApJ, 642, 382

Bromm, V., Yoshida, N., Hernquist, L., & McKee, C. F. 2009, Nature, 459, 49

Campisi, M. A., Li, L.-X., & Jakobsson, P. 2010, MNRAS, 407, 1972

Campisi, M. A., Maio, U., Salvaterra, R., & Ciardi, B. 2011a, MNRAS, 416, 2760

Campisi, M. A., Tapparello, C., Salvaterra, R., Mannucci, F., & Colpi, M. 2011b, MNRAS, 417, 1013

Chary, R., Berger, E., & Cowie, L. 2007, ApJ, 671, 272

Ciardi, B. & Loeb, A. 2000, ApJ, 540, 687

Conselice, C. J., Vreeswijk, P. M., Fruchter, A. S., et al. 2005, ApJ, 633, 29

de Souza, R. S., Yoshida, N., & Ioka, K. 2011, A&A, 533, A32

Falck, B. L., Riess, A. G., & Hlozek, R. 2010, ApJ, 723, 398

Frebel, A., Johnson, J. L., & Bromm, V. 2007, MNRAS, 380, L40

Granot, J., Panaitescu, A., Kumar, P., & Woosley, S. E. 2002, ApJ, 570, L61

Greif, T. H. & Bromm, V. 2006, MNRAS, 373, 128

Greif, T. H., Springel, V., White, S. D. M., et al. 2011, ApJ, 737, 75

Greiner, J., Hartmann, D. H., Voges, W., et al. 2000, A&A, 353, 998

Grindlay, J. E. 1999, ApJ, 510, 710

Hernquist, L. & Springel, V. 2003, MNRAS, 341, 1253

Hopkins, A. M. & Beacom, J. F. 2006, ApJ, 651, 142

Hosokawa, T., Omukai, K., Yoshida, N., & Yorke, H. W. 2011, Science, 334, 1250

Ioka, K. & Mészáros, P. 2005, ApJ, 619, 684

Ishida, E. E. O., de Souza, R. S., & Ferrara, A. 2011, MNRAS, 418, 500

Japelj, J. & Gomboc, A. 2011, PASP, 123, 1034

Jarosik, N., Bennett, C. L., Dunkley, J., et al. 2011, ApJS, 192, 14

Johnson, B. D. & Crotts, A. P. S. 2006, AJ, 132, 756

Johnson, J. L. & Bromm, V. 2006, MNRAS, 366, 247

Jordi, C., Gebran, M., Carrasco, J. M., et al. 2010, A&A, 523, 48

Kistler, M. D., Yüksel, H., Beacom, J. F., Hopkins, A. M., & Wyithe, J. S. B. 2009, ApJ, 705, L104

Komissarov, S. S. & Barkov, M. V. 2010, MNRAS, 402, L25

Kunszt, P. Z., Szalay, A. S., & Thakar, A. R. 2001, Mining the Sky: Proceedings of the MPA/ESO/MPE Workshop Held at Garching, 631

Kuznetsova, N. V. & Connolly, B. M. 2007, ApJ, 659, 530

Levesque, E. M., Kewley, L. J., Graham, J. F., & Fruchter, A. S. 2010, ApJ, 712, L26

Lindegren, L. 2009, Proc. IAU, 5, 296

Malacrino, F., Atteia, J.-L., Boër, M., et al. 2007, A&A, 464, L29

Mannucci, F., Buttery, H., Maiolino, R., Marconi, A., & Pozzetti, L. 2007, A&A, 461, 423

Mészáros, P. 2006, Reports on Progress in Physics, 69, 2259

Mészáros, P. & Rees, M. J. 2010, ApJ, 715, 967

Nagakura, H., Suwa, Y., & Ioka, K. 2011, arXiv:1104.5691

Nakar, E., Piran, T., & Granot, J. 2002, ApJ, 579, 699

Newling, J., Varughese, M., Bassett, B., et al. 2011, MNRAS, 414, 1987

Omukai, K., Tsuribe, T., Schneider, R., & Ferrara, A. 2005, ApJ, 626, 627

Ota, K., Iye, M., Kashikawa, N., et al. 2008, ApJ, 677, 12

Perna, R., Sari, R., & Frail, D. 2003, ApJ, 594, 379

Perryman, M. A. C., de Boer, K. S., Gilmore, G., et al. 2001, A&A, 369, 339

Poznanski, D., Maoz, D., & Gal-Yam, A. 2007, AJ, 134, 1285

Rau, A., Greiner, J., & Schwarz, R. 2006, A&A, 449, 79

Reddy, N. A., Steidel, C. C., Pettini, M., et al. 2008, ApJS, 175, 48

Richards, J. W., Homrighausen, D., Freeman, P. E., Schafer, C. M., & Poznanski, D. 2011, MNRAS, 1741

Robertson, B. E. & Ellis, R. S. 2012, ApJ, 744, 95

Rodney, S. A. & Tonry, J. L. 2009, ApJ, 707, 1064

Rossi, E. M., Perna, R., & Daigne, F. 2008, MNRAS, 390, 675

Rykoff, E. S., Aharonian, F., Akerlof, C. W., et al. 2005, ApJ, 631, 1032

Sako, M., Bassett, B., Connolly, B., et al. 2011, ApJ, 738, 162

Salvaterra, R. & Chincarini, G. 2007, ApJ, 656, L49

Salvaterra, R., Della Valle, M., Campana, S., et al. 2009, Nature, 461, 1258

Sari, R., Piran, T., & Halpern, J. P. 1999, ApJ, 519, L17

Sari, R., Piran, T., & Narayan, R. 1998, ApJ, 497, L17

Schneider, R., Ferrara, A., Natarajan, P., & Omukai, K. 2002, ApJ, 571, 30

Schneider, R., Ferrara, A., Salvaterra, R., Omukai, K., & Bromm, V. 2003, Nature, 422, 869

Sheth, R. K. & Tormen, G. 1999, MNRAS, 308, 119

Suwa, Y. & Ioka, K. 2011, ApJ, 726, 107

Toma, K., Sakamoto, T., & Mészáros, P. 2011, ApJ, 731, 127

Totani, T. 1997, ApJ, 486, L71

Totani, T. & Panaitescu, A. 2002, ApJ, 576, 120

Trenti, M. & Stiavelli, M. 2009, ApJ, 694, 879

Wang, F. Y. & Dai, Z. G. 2009, MNRAS, 400, L10

Woosley, S. E. & Bloom, J. S. 2006, ARA&A, 44, 507

Wyithe, J. S. B. & Loeb, A. 2003, ApJ, 586, 693

Yonetoku, D., Yamazaki, R., Nakamura, T., & Murakami, T. 2005, MNRAS, 362, 1114

Yoshida, N., Abel, T., Hernquist, L., & Sugiyama, N. 2003, ApJ, 592, 645

Yoshida, N., Oh, S. P., Kitayama, T., & Hernquist, L. 2007, ApJ, 663, 687

Yüksel, H., Kistler, M. D., Beacom, J. F., & Hopkins, A. M. 2008, ApJ, 683, L5